International Journal of Ocean System Engineering 1(1) (2011) 1-8
DOI 10.5574/IJOSE.2011.1.1.001

An experimental study on the hydro-elastic analysis of a circular cylindrical shell†

Cheon-hong Min[1], Han-il Park[1*], Bin Teng[2] and Byung-mo Kim[1]

[1] *Department of Ocean Engineering, Korea Maritime University, Dongsam-dong, Youngdo-gu, Busan 606-791, Korea*

[2] *State Key Laboratory of Coastal and Offshore Engineering, Dalian University of Technology, Dalian, 116024, China,*

(Manuscript Received December 17, 2010; Revised January 19, 2011; Accepted February 1, 2011)

Abstract

Ocean structures and vehicles are exposed to severe ocean environment conditions such as waves, winds and currents. When such ocean structures and vehicles are designed, an accurate structure analysis is required to keep the system safely. Hydro-elastic analysis is one of key issues to design such structures and vehicles. In many previous investigations, numerical analyses for hydro-elastic problem have been used. In this study, an experimental analysis is carried out and the circular cylindrical shell is considered. Dynamical characteristics for a circular cylindrical shell are identified by experimental vibration analysis in air and water. The natural frequencies and mode shapes are compared in air and water to obtain hydro-elastic effects. Some interesting results are found in the variation of natural frequencies and damping ratios of the circular cylindrical shell for different water contact depths.

Keywords: Circular cylindrical shell; Modal identification; Experimental modal analysis; Hydro-elastic analysis; Natural frequency and mode

1. Introduction

Ocean structures and vehicles are exposed to diverse sources of vibration, such as the vibration of the system itself or that from external load such as waves and wind. If the natural frequencies of an ocean structure and vehicles are close to the time varying external force applied to the structure or vehicle, it receives much damage due to much defection and fatigue on its structure. Research on the vibration characteristic of ocean structures and application of the knowledge to prevention of such harms are necessary.

The characteristic vibration of structures is expressed by system parameter such as natural frequency, damping ratio, mode shape, etc. These properties are decided by the quality of the material, shape, or environment conditions. Circular cylindrical shell structure is the most commonly used form in designing ocean structures and submarines. Therefore it is of great importance to investigate the vibration character of cylindrical shell structure which is in contact with water.

Many investigations have been carried out to analyze dynamic behavior of structures coupled with fluid. One of frequently employed methods for investigating the vibration character of structures is finite element method. In addition, in order to create a modeling for the studying contacting water effects on the structure, several methods such as, semi-analyical method, transfer matrix method and boundary element method are used.

Chen et al. (2003)[1] carried out nonlinear hydro-elastic analysis of a moored box-type floating body using the linear and nonlinear three-dimensional hydro-elastic equations. Ohkusu and Namba(2004)[2] carried out numerical analysis to predict the bending vibration of a very large floating structure of thin and

†This paper was presented at the Ninth International Society of Offshore and Polar Engineers(ISOPE) Pacific/Asia Offshore Mechanics Symposium, Busan, Korea, November 2010.

*Corresponding author. Tel.: +82-51-410-4326, Fax.: +82-51-403-4320.
E-mail address: hipark@hhu.ac.kr.

elongated rectangular plate configuration like a floating airport. Askari and Daneshmand (2009)[3] proposed finite element method using Galerkin method to analysis coupled vibration of a partially fluid-filled cylindrical container with a cylindrical internal body. Sigrist and Garreau (2007)[4] carried out finite element method in order to produce coupled fluid-structure dynamic analysis with pressure-based formulation, using modal and spectral method. Ugurlu and Ergin (2008)[5] investigated the effects of different end conditions on the response behavior of thin circular cylindrical shell structures fully in contact with flowing fluid using finite element and boundary element method.

Yet it is quite difficult to exactly predict the vibration character with these methods. Therefore to increase the accuracy of finite element model, some validations need to be performed through vibration experiments.

This research focuses on vibration experiments of a circular cylindrical shell structure in contact with water. By comparing the vibration characteristics of the cylindrical shell structure in air and water, it is expected to provide a proper method for interpreting vibration characteristics of ocean structures and submarines in partially contact with water.

2. Non-proportional damping system

The general equation of motion for a multi-degree-of-freedom (MDOF) system of N degrees of freedom with viscous damping is as follows:

$$[M]\{\ddot{x}\}+[C]\{\dot{x}\}+[K]\{x\}=\{f\} \tag{1}$$

where $[M]$, $[C]$, and $[K]$ are the $[N\times N]$ mass, damping, and stiffness matrices, and $\{x\}$ and $\{f\}$ are the $[N\times 1]$ vectors of the time-varying displacements and forces.

Free vibration is first considered to determine the natural frequencies and modes of the system. Next, a new coordinate vector $\{y\}$ that contains both displacements $\{x\}$ and velocities $\{\dot{x}\}$ vectors, is defined as follows:

$$\{y\}=\begin{Bmatrix} x \\ \dot{x} \end{Bmatrix}_{(2N\times 1)} \tag{2}$$

Then Eq. 1 can be rewritten for modal analysis in the following form.

$$[[C]:[M]]\{\dot{y}\}+[[K]:[0]]\{y\}=\{0\} \tag{3}$$

In this form, however, there are N equations and 2N unknowns. Thus it is necessary to add an identification equation of the following type:

$$[[M]:[0]]\{\dot{y}\}+[[0]:[-M]]\{y\}=\{0\} \tag{4}$$

Eq. 3 and 4 are combined to form a set of 2N equations.

$$\begin{bmatrix} [C] & [M] \\ [M] & [0] \end{bmatrix}\{\dot{y}\}+\begin{bmatrix} [K] & [0] \\ [0] & [-M] \end{bmatrix}\{y\}=\{0\} \tag{5}$$

This can be simplified to:

$$[A]\{\dot{y}\}+[B]\{y\}=\{0\} \tag{6}$$

The above equation leads to a standard eigen value problem, and a trial solution of the form $\{y\}=\{Y\}e^{st}$ can be assumed. The accelerance transfer function which is defined as acceleration response over force excitation for the non-proportional damping system is denoted by the following equation (Ewins, 2000)[6].

$$L(\omega)=\sum_{r=1}^{N}\left\{\frac{-\omega^2(U_r+jV_r)}{j(\omega-\omega_{dr})+\sigma_r}+\frac{-\omega^2(U_r-jV_r)}{j(\omega+\omega_{dr})+\sigma_r}\right\} \tag{7}$$

in which ω is a frequency, $\sigma_r=\omega_{nr}\varsigma_r$, ω_{nr} is an undamped natural frequency, ω_{dr} is a damped natural frequency, ς_r is a modal damping ratio, j is an imaginary unit and $U_r+jV_r=\phi_{ri}\phi_{rl}$, ϕ is an eigenvector. Usually, the frequency range of measurement is limited. Therefore, it is necessary to consider the residual terms as follows;

$$L(\omega)=\sum_{r=1}^{N}\left\{\frac{-\omega^2(U_r+jV_r)}{j(\omega-\omega_{dr})+\sigma_r}+\frac{-\omega^2(U_r-jV_r)}{j(\omega+\omega_{dr})+\sigma_r}\right\}+C+jD-\omega^2E-j\omega^2F \tag{8}$$

in which parameter C and D are respectively real and imaginary parts of the residual mass, E and F are respectively real and imaginary parts of the residual stiffness.

3. Non-linear least squares method

In Eq. 8, the coefficients $\omega_{dr},\sigma_r,U_r,V_r,C,D,E,F$ are unknown factors and are denoted by parameter $\gamma_h(h=1\sim 4N+4)$. Eq. 8 is not linear and thus the parameters cannot be directly obtained from it. If ω_{dr} and σ_r are known, however, Eq. 8 can be solved directly. In this study, the approximate values of ω_{dr} and σ_r were obtained using a half-power bandwidth method. Then the NLLS method was used to define the other parameters such as U_r,V_r,C,D,E,F. In addition, their initial values were denoted by parameter γ_{hs}.

$$\gamma_h = \gamma_{hs} + \Delta\gamma_h \tag{9}$$

Eq. 10 below is the Tayler series of Eq. 9 expanded by $\Delta\gamma_h$.

$$L(\omega,\gamma_h) \cong L(\omega,\gamma_{hs}) + \sum_{h=1}^{4N+4} \frac{\partial L}{\partial \gamma_h}(\omega,\gamma_{hs}) \bullet \Delta\gamma_h = A_{\mathrm{Re}} + jA_{\mathrm{Im}} \tag{10}$$

in which $\frac{\partial L}{\partial \gamma_h}$ is denoted by:

$$\begin{aligned}
\frac{\partial L}{\partial \omega_{dr}} &= \frac{-j\omega^2(U_r+V_r)}{\{j(\omega-\omega_{dr})+\sigma_r\}^2} + \frac{j\omega^2(U_r-V_r)}{\{j(\omega+\omega_{dr})+\sigma_r\}^2} \quad (r=1\sim N)\\
\frac{\partial L}{\partial \sigma_r} &= \frac{\omega^2(U_r+jV_r)}{\{j(\omega-\omega_{dr})+\sigma_r\}^2} + \frac{\omega^2(U_r-jV_r)}{\{j(\omega+\omega_{dr})+\sigma_r\}^2} \quad (r=1\sim N)\\
\frac{\partial L}{\partial U_r} &= \frac{-\omega^2}{j(\omega-\omega_{dr})+\sigma_r} + \frac{-\omega^2}{j(\omega+\omega_{dr})+\sigma_r} \quad (r=1\sim N)\\
\frac{\partial L}{\partial V_r} &= \frac{-j\omega^2}{j(\omega-\omega_{dr})+\sigma_r} + \frac{j\omega^2}{j(\omega+\omega_{dr})+\sigma_r} \quad (r=1\sim N)\\
\frac{\partial L}{\partial C} &= 1, \quad \frac{\partial L}{\partial D} = j, \quad \frac{\partial L}{\partial e} = -\omega^2, \quad \frac{\partial L}{\partial F} = -j\omega^2
\end{aligned} \tag{11}$$

The measurement data are denoted by L_{Re} and L_{Im}. On the other hand, the theoretical data are denoted by A_{Re} and A_{Im}. The error function is defined as τ.

$$\tau = \sum_{i=1}^{m} \left\{ (L_{\mathrm{Re}i} - A_{\mathrm{Re}i})^2 + (L_{\mathrm{Im}i} - A_{\mathrm{Im}i})^2 \right\} \tag{12}$$

The error function needs to be minimized. This can be achieved by differentiating Eq.12 by $\Delta\gamma_h$.

$$\frac{\partial \tau}{\partial \Delta\gamma_h} = 2\sum_{i=1}^{m} \left\{ \frac{\partial A_{\mathrm{Re}i}}{\partial \Delta\gamma_h}(A_{\mathrm{Re}i} - L_{\mathrm{Re}i}) + \frac{\partial A_{\mathrm{Im}i}}{\partial \Delta\gamma_h}(A_{\mathrm{Im}i} - L_{\mathrm{Im}i}) \right\} = 0 \tag{13}$$

Eq. 13 is transposed simultaneously with $[(4N+4)\times(4N+4)]$. Finally, the values of γ_h are obtained by simultaneously solving the equations.

4. Experimental procedures

To understand the vibration characteristics of a circular cylindrical shell in air and water, experiments were performed for three different contact conditions with water. The selected material of the circular cylindrical shell is stainless steel, and its dimension and properties are given in Table 1.

Table 1. Dimension and properties of circular cylindrical shell used in experiment

Outer radius	0.250 m
Inner radius	0.248 m
Thickness	0.002 m
Length	1.5 m

Experiments on the vibration analysis of a semi-submerged circular cylindrical shell was performed in 2-dimentional wave tank of height 1.5m, width 1m, length 25m. The water tank is large enough relative to the size of circular cylindrical shell to eliminate effects due to restrictions of the surface of walls. Circular cylindrical shell was hung by thin chains connected to two points on both shell ends, and the surface area in contact with water was controlled by adjusting the length of chain.

To carry out the modal analysis, one acceleration sensor was mounted on one point on the circular cylindrical shell, and average value was acquired by vibrating twice the 8 points marked longitudinally on the circular cylindrical shell with a shock hammer. FFT analyzer used in the experiment was B&K's 2 channel 3560B. Fig 1 shows the set-up of the equipment.

This experiment is to investigate the vibration characteristics of a cylindrical shell in air and water with two different contact depths. To do so, firstly the circumference of the circular cylindrical shell surface is divided into 16 pieces of equal angle, and for every piece, 8 points are marked longitudinally. In other words, on the surface of circular cylindrical shell 16 lines are drawn, and for every line 8 points are marked, as shown in Fig. 2. After hanging the marked circular cylindrical shell in the air to meet the free

boundary condition, acceleration censor is attached on the shell and free vibrations are generated by impacting on 32 points by using a shock hammer.

Fig. 3 shows the circular cylindrical shell in contact with water by 1/4 of its total surface, and Fig. 4 shows the circular cylindrical shell in contact by 1/3 of its total surface. Afterwards, an accelerator censor is attached on the point with same free surface condition in the air that was not semi-submerged, and the experiment was performed under the same procedure.

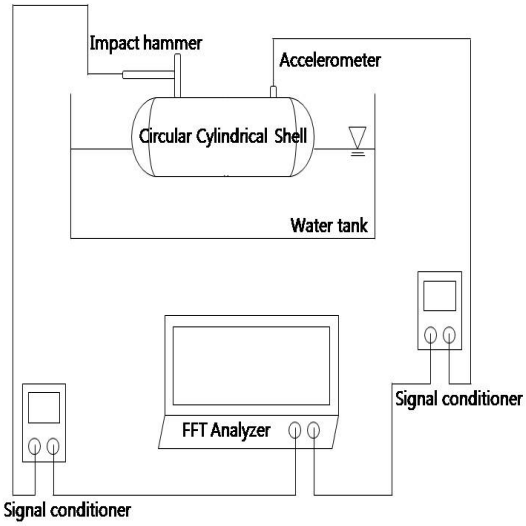

Fig.1 Schematics of Experimental Set-up

Fig.2 Points of the circular cylindrical shell marked on the surface

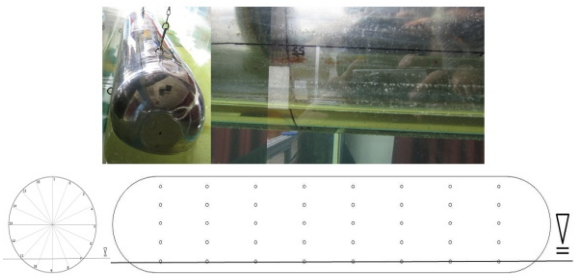

Fig.3 The shapes of circular cylindrical shell of which 1/4 of circumference semi-submerged under water

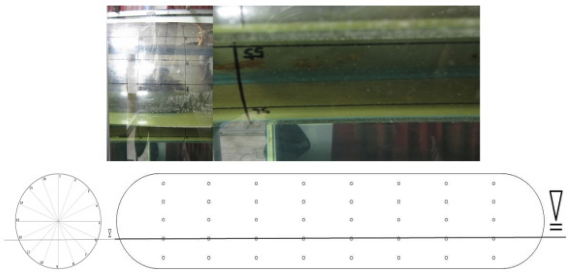

Fig.4 The shapes of circular cylindrical shell of which 1/3 of circumference semi-submerged under water

5. Results and discussion

Figs 5~7 is drawn by overlaying transfer functions on each point in air, 1/4 semi-submerged, and 1/3 semi-submerged, respectively. It can be seen that the structure's number of resonance frequency differs according to the area semi-submerged. Of these, modes excluding the low-dimensional modes created by constraints and rigid body modes were used for curve-fitting. In this research NLLS method was used for curve-fitting method. Specific procedures for curve-fitting are introduced in the reference (Min et al. 2008, Min et al. 2009)[7][8]. Fig. 8 overlays and compares the experimentally measured plot and curve-fitted plot of the circular cylindrical shell in air when impacted on the fifth point. Fig. 9 overlays and compares the experimentally measured plot with curve-fitted frequency transfer function when the circular cylindrical shell is 1/4 semi-submerged and vibrated on the same point. Fig. 10 overlays and compares the result of vibration on the same point with curve-fitted frequency transfer function when the circular cylindrical shell is 1/3 semi-submerged.

Table 2 shows identified natural frequencies of cylindrical shell in air, 1/4 semi-submerged, and 1/3 semi-submerged, respectively. Since natural frequencies are changed according to semi-submerged conditions, it needs to compare mode shapes for each condition in order to obtain vibration parameters for different semi-submerged condition.

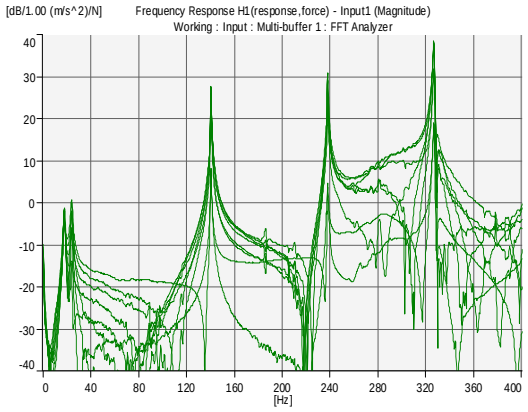

Fig.5 Transfer functions measured at each point of the circular cylindrical shell in air

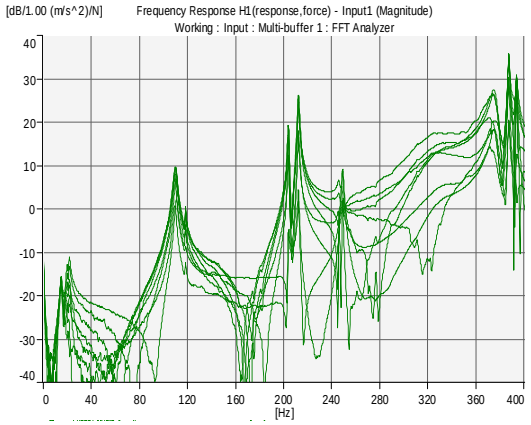

Fig.6 Transfer functions measured at each point of the circular cylindrical shell of which 1/4 semi-submerged

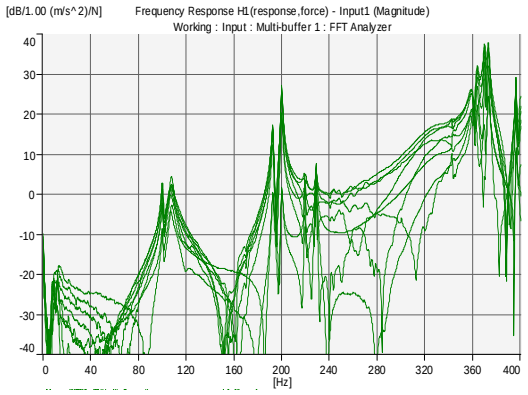

Fig.7 Transfer functions measured at each point of the circular cylindrical shell of which 1/3 semi-submerged

Table 2. Identified natural frequencies of circular cylindrical shell

	In the air	1/4 semi-submerged	1/3 semi-submerged
1st mode	140.0783 Hz	203.5060 Hz	192.4941 Hz
2nd mode	237.6622 Hz	212.0008 Hz	199.8336 Hz
3rd mode	326.2227 Hz	248.7578 Hz	219.1898 Hz
4th mode		326.7155 Hz	228.5245 Hz
5th mode		375.0504 Hz	325.8649 Hz
6th mode		386.7561 Hz	359.9016 Hz
7th mode		393.0831 Hz	363.2449 Hz
8th mode			369.5623 Hz
9th mode			372.7864 Hz
10th mode			395.8568 Hz

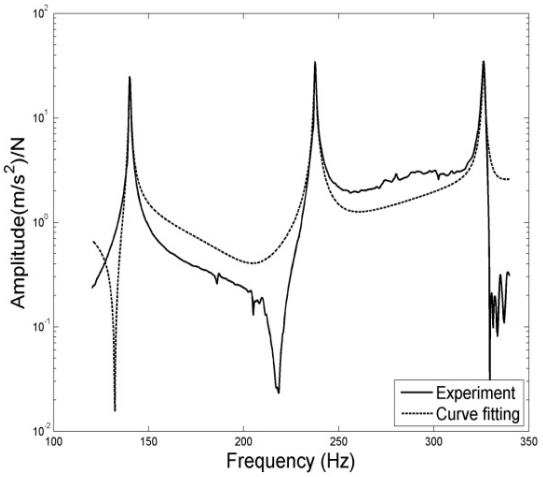

Fig.8 Comparison of the experimentally measured plot and curve-fitted plot of the circular cylindrical shell in air

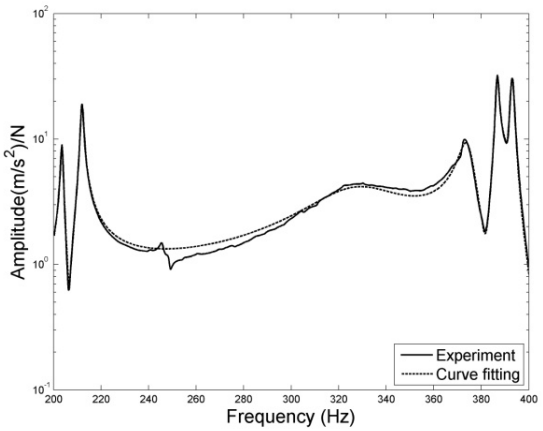

Fig.9 Comparison of the experimentally measured plot and curve-fitted plot of the circular cylindrical shell of which 1/4 semi-submerged

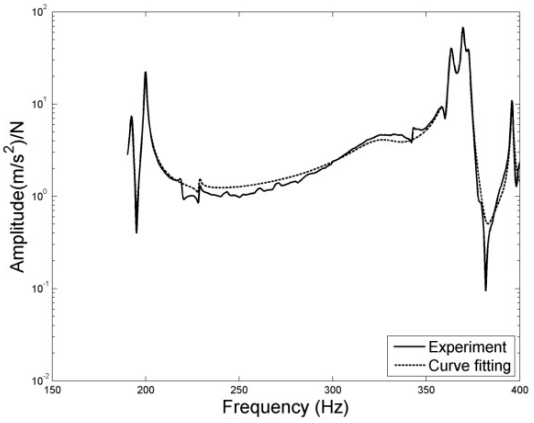

Fig.10 Comparison of the experimentally measured plot and curve-fitted plot of the circular cylindrical shell of which 1/3 semi-submerged

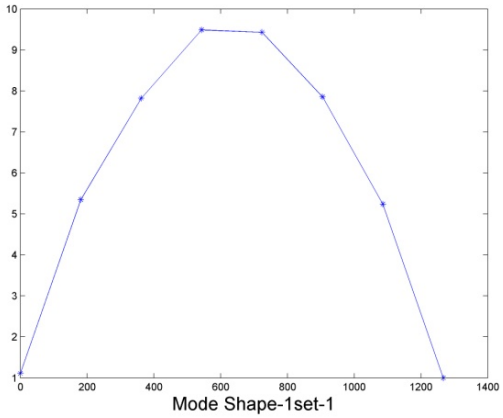

Fig.11 Standard mode shape 1

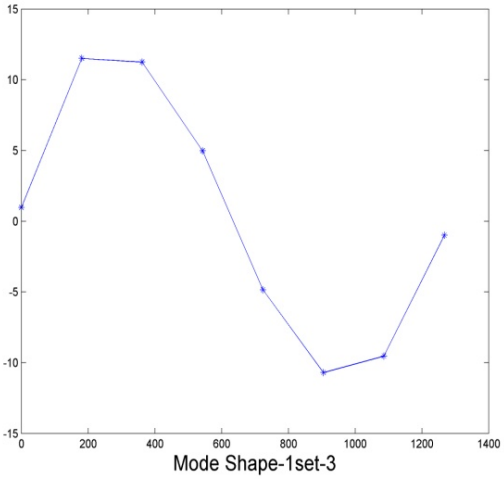

Fig.12 Standard mode shape 2

Fig. 11 and Fig. 12 are mode shapes selected as a standard for comparison among mode forms derived from data analysis by curve-fitted frequency transfer functions.

MAC(Modal Assurance Criterion) values are calculated in order to compare standard mode shapes to 1/3 and 1/4 semi-submerged mode shapes. MAC is defined as Eq. 14.

$$MAC\left(\{\phi_X\}_i, \{\phi_A\}_j\right) = \frac{\left|\{\phi_X\}_i^T \{\phi_A^*\}_j\right|^2}{\left(\{\phi_X\}_i^T \{\phi_X^*\}_i\right)\left(\{\phi_A\}_j^T \{\phi_A^*\}_j\right)} \quad (14)$$

Where, ϕ_X and ϕ_A are the mode shape at X and A, respectively. i, j are the ith and jth mode shape, respectively. If mode shapes at X and A are in fact same, a value of the MAC is close to 1.0, whereas if they are actually not related each other, values close to 0. Figs. 13~16 show MAC values.

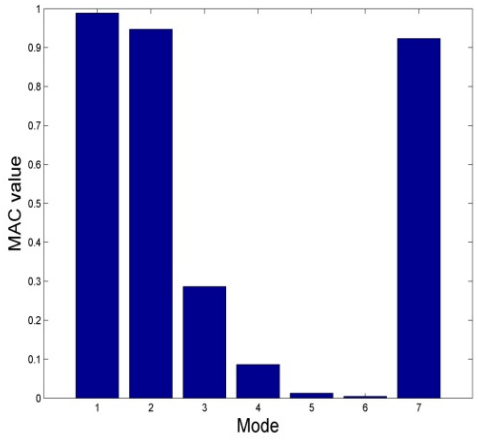

Fig.13 MAC values of standard mode shape 1 and 1/4 semi-submerged mode shapes

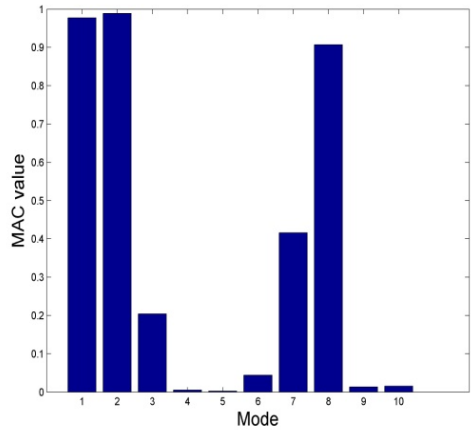

Fig.14 MAC values of standard mode shape 1 and 1/3 semi-submerged mode shapes

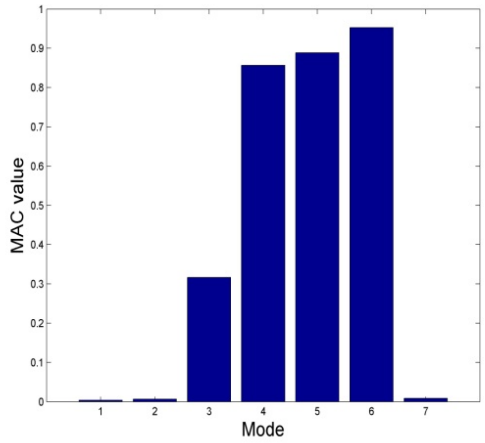

Fig.15 MAC values of standard mode shape 2 and 1/4 semi-submerged mode shapes

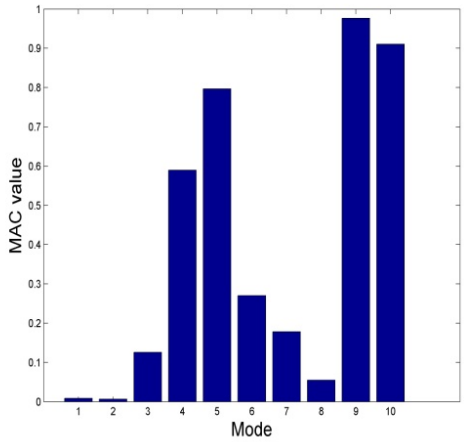

Fig.16 MAC values of standard mode shape 2 and 1/3 semi-submerged mode shapes

Table 3. Natural frequencies corresponding to standard mode shapes in air and semi- submerged

	Standard mode shape 1	Standard mode shape 2
In the air	140.0783 Hz	326.2227 Hz
1/4 semi-submerged	203.5060 Hz	386.7561 Hz
1/3 semi-submerged	199.8336 Hz	372.7864 Hz

Natural frequency of mode shape of Fig. 11 in the air is 140.0784Hz, and the natural frequency of mode shape of Fig. 12 is 326.222Hz. When the circular cylindrical shell is 1/4 semi-submerged, mode shape takes form of Fig. 11 when natural frequency is 204.5060Hz, and takes form of Fig. 12 when natural frequency is 386.7561Hz. When circular cylindrical shell is 1/3 semi-submerged underwater, mode shape takes form of Fig. 11 when natural frequency is 199.8336Hz, and takes form of Fig. 12 when natural frequency is 372.7864Hz.

Table 4. Modal damping ratio corresponding to standard mode shapes in air and semi-submerged

	Standard mode shape 1	Standard mode shape 2
In the air	0.00213	0.001
1/4 semi-submerged	0.00221	0.00161
1/3 semi-submerged	0.00228	0.00234

Table 3 shows the comparison of natural frequencies of mode 1 and 2 for the cylindrical shell in air, 1/4 semi-submerged, and 1/3 semi-submerged. It can be seen that the natural frequencies of semi-submerged cases are relatively much higher compared to those of the circular cylindrical shell in the air. The reason is that when the shell is semi-submerged, added mass occurs and induces the natural frequency to be smaller but buoyancy is also occurred and makes the vibration stiffness to be increased. In this case, the stiffness effect on the increase of natural frequencies is larger than that of added mass.

From Table 3, it can be seen that the natural frequencies of the circular cylindrical shell in 1/3 semi-submerged is slightly smaller than those of 1/4 semi-submerged case. The reason is that if the cylindrical shell is more semi-submerged, the effect of added mass is larger than that of buoyancy induced stiff.

Table 4 shows modal damping ratio for each standard mode shape. It is seen that modal damping ratio corresponding to the first mode in Fig. 11 has relatively decreased compared to the modal damping ratio of the second mode in Fig. 12. The modal damping ratio of the cylindrical shell in air is relatively small compared to that of semi-submerged case. And the damping ratio increases as the semi-submerged depth increases.

6. Conclusions

In this research, an experiment was carried out to investigate the vibration characteristics of a circular cylindrical shell in air and semi-semi-submerged

condition. The natural frequencies and mode shapes are compared in air and water to obtain hydro-elastic effects. It was found that for the same mode the natural frequency of the cylindrical shell in semi-submerged case is greater than that in air. The reason is that the effect of buoyancy on the increase of natural frequency is greater than that of added mass. If submergence depth is increased, the natural frequency is slightly decreased. The modal damping ratio of the cylindrical shell in air is relatively small compared to that of semi-submerged case.

Acknowledgements

This research was a part of the project titled "Development of Key Marine Equipments for Enhancement of Ocean Industry - Development of Underwater Manipulator and Thrusting System Driven by Electric Motor" funded by the Ministry of Land, Transport and Maritime Affairs, Korea.

References

[1] Chen, X, Wu, Y, Cui, W, and Tang, X (2003). "Nonlinear Hydroelastic Analysis of a Moored Floating Body", Ocean Engineering, Vol 30, pp 965-1003.

[2] Ohkusu, M, and Namba, Y (2004). "Hydroelastic Analysis of a Large Floating Structure", Journal of Fluids and Structures, Vol 19, pp 543-555.

[3] Askari, E, and Daneshmand, F (2009). "Coupled Vibration of a Fluid-Filled Cylindrical Container with a Cylindrical Internal Body", Journal of Fluids and Structures, Vol 25, pp 389-405.

[4] Sigrist, JF, and Garreau, S (2007). "Dynamic Analysis of Fluid-Structure Interaction Problems with Modal Methods using Pressure-based Fluid Finite Elements", Finite Elements in Analysis and Design, Vol 43, pp 287-300

[5] Ugurlu, B, and Ergin, A (2008). "A Hydroelastic Investigation of Circular Cylindrical Shells-containing Flowing Fluid with Different End Conditions", Journal of Sound and Vibration, Vol 318, pp 1291-1312.

[6] Ewins, DJ (2000). "Modal Testing 2," Research Studies Press Ltd.

[7] Min, CH, Park, HI, and Bae, SR (2008). "Experimental Vibration Analysis of Damped Beam Model Using Multi-degree Curve Fitting Method", Journal of Ocean Engineering and Technology, KSOE, Korea, Vol 22, No 1, pp 70-74.

[8] Min, CH, Park, HI, Bae, SR, and Jeon, JJ (2009). "New Global Curve Fitting Method Using Frequency Response Function", Journal of Ocean Engineering and Technology, KSOE, Korea, Vol 23, No 6, pp 82-86.